

Optimising the Focus Tube Length for Abrasive Water Jet Using Numerical Simulations

by

**Dewan Hasan Ahmed
Rowan Deam, (IRIS)
Jamal Naser, (Swinburne University of Technology)
Frank Chen, (IRIS)**

Abstract

This research was undertaken within IRIS at the Swinburne University of Technology and the funding for this research program was obtained from the Australian Research Council. This project commenced in August 2000 and the expected completion date is August 2003. This paper addresses the optimisation of focus tube length for the abrasive water jet which is used as a modern industrial cutting technique.. Numerical simulations of the abrasive water jet have been carried out and a Computational Fluid Dynamics (CFD) model has been developed to optimise the focus tube geometry. The study has been carried out using a multi-phase approach. The governing equations were discretized using the finite volume approach. The solution was obtained using the Inter-Phase Slip Algorithm (IPSA). The governing equations were closed using the K- ϵ turbulence model. The model predicted a significant effect of the focus tube length on jet velocities at the exit of the nozzle assembly. Simulated results were compared with experimental results by measuring the jet strike force for different water pressure levels. The results show agreement with the experimental data.

1. Introduction

The focus tube in a water jet cutting system accelerates the abrasive particles used for cutting. This is a critical role. The faster the abrasive jets the better. Abrasive jets are made up of three continuous phases: solid, water and air and are much more complex than plain water jets. The velocity distribution in abrasive water jet for precision cutting is also a very important parameter. Experimental investigations for finding the velocity of water and abrasive particles have been obtained using two different methods. Many researchers have ignored air, probably because it is difficult to measure the velocity of air at the exit of the focus tube. Scharner (1998) calculated the air flow rate according to the abrasive flow rate. It is clear from the paper that the geometry of the mixing chamber has a great influence on the air flow rate. Neusen (1994) showed from an experimental study that at 4mm stand-off distance, the composition of abrasive water jet on a volume basis is approximately 4% to 6% water, 0.2% to 0.5% abrasive and 93% to 95% air. Tazibt (1996) showed that the air sucked in with the abrasive particles occupies more than 90% of the volume of an abrasive water jet, and hence it has a great

influence on the abrasive water jet process. In this research we have simulated the abrasive water jet by considering three phases for conventional entrainment jets. The CFD software CFX-4 was used for these simulations. Water and solid was considered to be incompressible and air as compressible. The simulations were carried out for steady state, turbulent flow with heat transfer. Water was considered as the primary phase and abrasive and air as secondary phases.

2. Industrial Implications

The main aspects of abrasive water jet machining (AWJM) are the possible range of work materials and the possible ranges of product shape and product accuracy. The main advantages of AWJM are the low temperature and the low forces on the work piece. It is hoped that a better understanding of the three phase mixing process will lead to improved AWJ mixing assembly designs in a way which would increase the efficiency of the energy transfer from water to the particles. The desired outcomes would be reduced mixing tube wear, abrasive particle size breakdown, and increased particle speeds. These outcomes would translate into increased cutting speed, improved surface quality and lower operating costs.

2. Mathematical Modelling

Governing equations were solved for the time averaged values of the velocity components, pressure, volume fractions and turbulence parameters. The equations, represented below, were closed using the k- ϵ turbulence model. The three phases were labelled by Greek indices α , β and γ representing water, air and solid respectively. The volume fraction of each phase is denoted r_α . The subscript α denotes the phase water and the equations for air and solid phases can be obtained by replacing α with β and γ respectively.

The continuity equation

$$\nabla \cdot (r_\alpha \rho_\alpha \mathbf{U}_\alpha) = 0 \quad (1)$$

The momentum equation

$$\nabla \cdot \left\{ r_\alpha \left[\rho_\alpha \mathbf{U}_\alpha - \mu_{\text{eff}} (\nabla \mathbf{U}_\alpha + (\nabla \mathbf{U}_\alpha)^T) \right] \right\} = r_\alpha (\mathbf{B} - \nabla p_\alpha) + \sum_{\beta=1}^{N_p} c_{\alpha\beta}^{(d)} (\mathbf{U}_\alpha - \mathbf{U}_\beta) + \mathbf{F}_\alpha \quad (2)$$

where N_p is the no. of phases.

$$\text{Where } \mu_{\text{eff}} = \mu_\alpha + \mu_{T\alpha} \quad (3)$$

μ_{eff} , μ_α and $\mu_{T\alpha}$ is the effective, molecular and turbulent viscosity respectively.

$$\text{and } \mu_{T\alpha} = C_\mu \rho_\alpha \frac{k_\alpha^2}{\epsilon_\alpha} \quad (4)$$

Here k is the turbulence kinetic energy and ϵ is the dissipation length scale.

The energy equation

$$\nabla \cdot [r_\alpha (\rho_\alpha \mathbf{U}_\alpha H_\alpha - \lambda_\alpha \nabla T_\alpha)] = \sum_{\beta=1}^{N_p} c_{\alpha\beta}^{(h)} (T_\beta - T_\alpha) \quad (5)$$

The general advection-diffusion equation is:

$$\nabla \cdot [r_\alpha (\rho_\alpha \mathbf{U}_\alpha \Phi_\alpha - \Gamma_\alpha \nabla \Phi_\alpha)] = r_\alpha S_\alpha + \sum_{\beta=1}^{N_p} c_{\alpha\beta} (\Phi_\beta - \Phi_\alpha) \quad (6)$$

The term $c_{\alpha\beta} (\Phi_\beta - \Phi_\alpha)$ describes inter-phase transfer of Φ between α and β .

Equation of volume fraction

$$\nabla \cdot (r_\alpha \rho_\alpha \mathbf{U}_\alpha - \Gamma_\alpha \nabla r_\alpha) = 0 \quad (7)$$

where $\Gamma_\alpha = \frac{\mu_{T\alpha}}{\sigma_\alpha}$ and σ_α is the turbulent Prandtl number. The turbulent dispersion of volume fraction was modelled using the Eddy diffusivity hypothesis.

The transport equation for k and ϵ takes the same form as the generic scalar advection-diffusion equation

$$\nabla \cdot \left\{ r_\alpha \left[\rho_\alpha \mathbf{U}_\alpha k_\alpha - \left(\mu + \frac{\mu_{T\alpha}}{\sigma_k} \right) \nabla k_\alpha \right] \right\} = r_\alpha S_{k\alpha} + \sum_{\beta=1}^{N_p} c_{\alpha\beta}^{(k)} (k_\beta - k_\alpha) \quad (8)$$

$$\nabla \cdot \left\{ r_\alpha \left[\rho_\alpha \mathbf{U}_\alpha \epsilon_\alpha - \left(\mu + \frac{\mu_{T\alpha}}{\sigma_\epsilon} \right) \nabla \epsilon_\alpha \right] \right\} = r_\alpha S_{\epsilon\alpha} + \sum_{\beta=1}^{N_p} c_{\alpha\beta}^{(\epsilon)} (\epsilon_\beta - \epsilon_\alpha) \quad (9)$$

The source terms were considered to be the same as their single-phase analogies and thus:

$$S_{k\alpha} = P_\alpha - \rho_\alpha \epsilon_\alpha \quad (10)$$

$$S_{\epsilon\alpha} = \frac{\epsilon_\alpha}{k_\alpha} (C_{1\epsilon} P_\alpha - C_{2\epsilon} \rho_\alpha \epsilon_\alpha) \quad (11)$$

where P_α is the shear production. The constants were set as

$$C_\mu = 0.09, C_1 = 1.44, C_2 = 1.92, \sigma_k = 1.00 \text{ and } \sigma_\epsilon = 1.217$$

Air was considered as compressible; its density was calculated from the ideal gas law:

$$\rho = \frac{pW}{RT} \quad (12)$$

where $p = P + P_{ref}$. Here W , R , P and T denote the molecular weight, universal gas constant, pressure and temperature respectively.

3. Geometry and Parameters

The cylindrical coordinate system was used to create the geometry for the conventional entrainment jet. A schematic of the abrasive water jet nozzle is shown in Figure 1. An atmospheric pressure boundary condition was applied to the nozzle exit. The geometrical parameters and other boundary conditions are shown in Table 1.

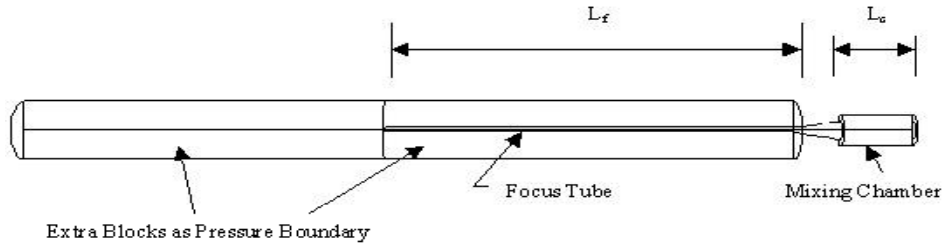


Figure 1. Schematic diagram of AWJ nozzle

Nozzle dimensions		
Orifice diameter		0.33 mm
Mixing chamber diameter		6.5 mm
Mixing chamber length, L_c		12 mm
Focus tube diameter		1.016 mm
Abrasive inlet diameter		4 mm
Abrasive density		4100 kg/m ³
Abrasive diameter		180 μ m
Inlet conditions		
Water pressure		276 MPa
Air pressure		0.76 MPa
Abrasive mass flow rate		0.45 kg /min
Air flow rate		2.67 lit/min

Table 1. Geometry parameters and boundary conditions

4. Results and Discussions

To determine the effect of the focus tube length on jet velocity, simulations were carried out for different focus tube lengths (55mm, 67.5mm, 75mm, 85mm, 95mm and 105mm). Ahmed (2001) showed that for the taper inlet angle of 75° the velocity of the different phases were higher compared with that of the other taper inlet angles. Here, the simulations were carried out for the taper inlet angle of 75° for different focus tube lengths. The average velocities at the exit near the central axis region for different focus tube lengths are shown in Figure 2. The average velocity increases up to an optimum and then decreases with further increases of the focus tube length. The exit velocities of different phases near the central axis region for the different focus tube lengths are shown in Figure 3. The exit velocity trend for different focus tube lengths shows that there is one focus tube length is necessary for getting the maximum velocity. The velocity distribution along the focus tube length for different radial positions. Figures 4 and 5 show the average velocities as a function of focus tube length (95mm) at 0.1058mm and 0.2328mm from the centre of the tube.

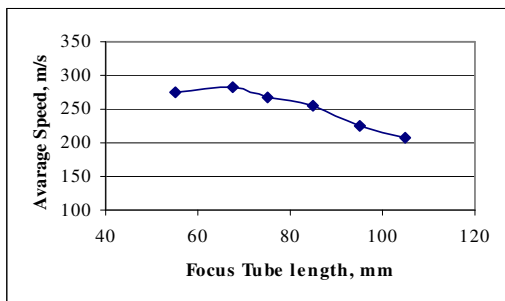


Figure 2 – Average Jet Speed at Exit of Focus Tube for Different Tube Lengths

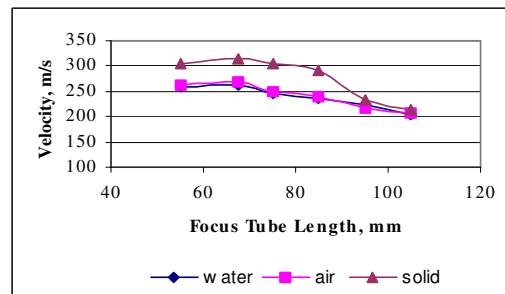


Figure 3 – Exit Velocity of Different Phases Near Central Axis Region for Different Tube Lengths

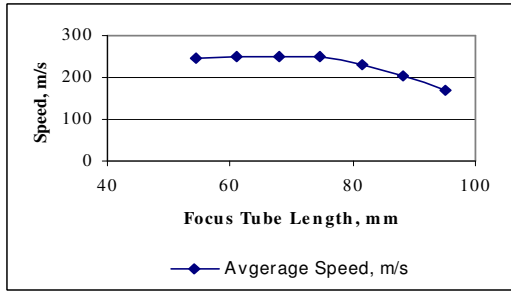


Figure 4 – Average Speed at a Radius of 0.1058mm from Tube Centre

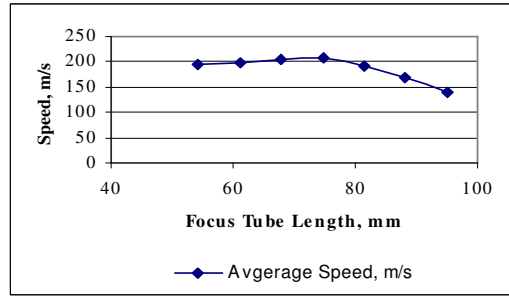


Figure 5 – Average Speed at a Radius of 0.2328mm from Tube Centre

It was determined that the optimum focus tube length was approximately 75mm. For focus tube lengths longer than 75mm the jet velocity decreased quickly. Ye and Kovacevic (1999) showed that when the focus tube length is small the jets don't have enough time to accelerate, but when the focus tube length is too long the abrasive particles slow down. This is because, with the increase in focus tube length, there are more chances of collision between the particles and the tube wall.

5. Validation of the Simulation

A force transducer was used to measure the jet striking force for an unpenetrated cut. The results were used to validate the model. Figure 6 shows the standard measuring chain that was used to measure the Y and Z direction forces. A 10 mm thick mild-steel plate was used as test specimens and jet strike forces were measured. All experiments were completed for the 20 sample readings per second averaged over 5 seconds. The forces were measured for three different stand-off distances and for three different pressures. The simulations were carried out for three different water pressures. The forces were calculated from the pressure and the velocity near the solid surface. The predicted forces at a 4mm stand-off distance are compared with the experimental results in Figure 7. The predicted and experimental data were in agreement.

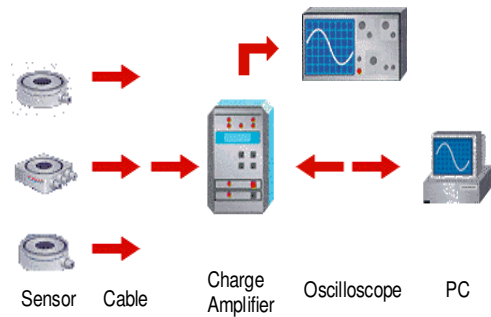


Figure 6 Standard Measuring Chains

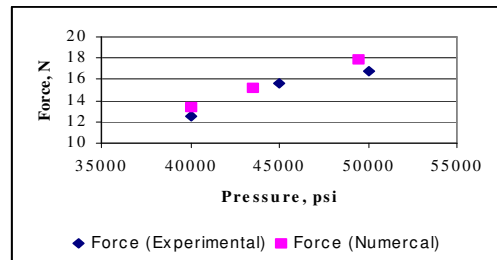


Figure 7 – Jet Strike Force for Different Water Pressures at 4mm Stand-off Distance

6. Conclusions

- ◆ A CFD model of the focus tube for water jet cutting has been developed and tested against experiments.
- ◆ The model was used to predict an optimum focus tube length of 75mm for the conditions modelled.

7. Acknowledgments

The authors would like to thank the Australian Research Council (ARC) for the support of this work.

8. References

Ahmed, D. H., Siores, E., Naser, J., and Chen, F. L., "Numerical Simulation of Abrasive water jet for Different Taper Inlet Angle", Proceedings of the Fourteenth Australasian Fluid Mechanics Conference, Adelaide, Australia, Vol. 2, pp645-648, 2001.

Neusen, K. F., Gores, T. J., and Amano, R. S., "Axial Variation of Particle and Drop Velocities Downstream From an Abrasive Water Jet Mixing Tube," 12th International Symposium on Jet Cutting Technology, pp93-103, 1994.

Scharner, M., Weseslindtner, H., Trieb, F., Herbig, N., and Haase, C., "Study on the Influence of Mixing Chamber Dimensions in Abrasive Waterjet Cutting Heads on Cutting Efficiency," 14th International Conference on Jetting Technology, BHR Group Conference Series, Publication No. 32, pp169-183, 1998.

Tazibt, A. Q., Parsy, F., and Abriak, N., "Theoretical Analysis of the Particle Acceleration Process in Abrasive Water Jet Cutting," Computational Material Science, Vol. 5, pp243-254, 1996.

Ye, J., and Kovacevic, R., "Turbulent Solid-Liquid Flow Through the Nozzle of Premixed Abrasive Water Jet Cutting System," Proc. Instn Mech Engineers, Vol.213, Part B, pp59-67, 1999.